

## ORIGINAL ARTICLE

# Orthotopic tracheal transplantation using human bronchus: an original xenotransplant model of obliterative airway disorder

Julien Guihaire<sup>1,2</sup>, Ryo Itagaki<sup>1,2</sup>, Mandy Stubbendorff<sup>1,2</sup>, Xiaoqin Hua<sup>1,2</sup>, Tobias Deuse<sup>1,2,3,8</sup>, Sebastian Ullrich<sup>4</sup>, Elie Fadel<sup>5</sup>, Peter Dorfmueller<sup>6</sup>, Robert C. Robbins<sup>7</sup>, Hermann Reichenspurner<sup>2,3</sup>, Udo Schumacher<sup>4</sup> & Sonja Schrepfer<sup>1,2,7,8</sup>

1 TSI-Laboratory, University Heart Center Hamburg, Hamburg, Germany

2 Cardiovascular Research Center Hamburg (CVRC) and DZHK (German Center for Cardiovascular Research), Partner Site Hamburg/Kiel/Luebeck, Hamburg, Germany

3 Cardiovascular Surgery, University Heart Center Hamburg, Hamburg, Germany

4 Department of Anatomy and Experimental Morphology, University Hospital Hamburg-Eppendorf, Hamburg, Germany

5 Thoracic and Vascular Surgery and Heart-Lung Transplantation, Marie Lannelongue Hospital, University of Paris Sud, Le Plessis Robinson, France

6 Department of Pathology, Marie Lannelongue Hospital, University of Paris Sud, Le Plessis Robinson, France

7 Department of Cardiothoracic Surgery, Cardiovascular Institute, Stanford University School of Medicine, Stanford, CA, USA

8 University of California San Francisco (UCSF) Department of Surgery, Division of Cardiothoracic Surgery, Transplant and Stem Cell Immunobiology (TSI), Lab San Francisco, CA, USA

## Correspondence

Sonja Schrepfer, Transplant and Stem Cell Immunobiology Lab (TSI), University Heart Center Hamburg, Martinistraße 52, Campus Research, N27, room 068, 20246 Hamburg, Germany.  
Tel.: +49-40-74105-9982;  
fax: +49-40-74105-9663;  
e-mail: sonja.schrepfer@ucsf.edu

J.G. and R.I. share first-authorship.  
U.S. and S.S. share last authorship.

[Correction added on 13 October 2016 after first online publication: Author affiliations have been corrected in this version.]

## SUMMARY

Bronchiolitis obliterans syndrome (BOS) is a main cause of allograft dysfunction and mortality after lung transplantation (LTx). A better understanding of BOS pathogenesis is needed to overcome this treatment-refractory complication. Orthotopic tracheal transplantation using human bronchus was performed in Brown Norway (BN) and nude (RNU) rats. Allografts were recovered in both strains at Day 7 (BN<sub>7</sub>, *n* = 6; RNU<sub>7</sub>, *n* = 7) or Day 28 (BN<sub>28</sub>, *n* = 6; RNU<sub>28</sub>, *n* = 6). Immune response of the host against the bronchial graft was assessed. Human samples from BOS patients were used to compare with the histological features of the animal model. Obstruction of the allograft lumen associated with significant infiltration of CD3+ and CD68+ cells was observed in the BN group on Day 28. Immune response from type 1 T-helper cells against the tracheal xenograft was higher in BN animals compared to nude animals on Days 7 and 28 (*P* < 0.001 and *P* = 0.035). Xenoreactive antibodies were significantly higher at Day 7 (IgM) and Day 28 (IgG) in the BN group compared to RNU (respectively, 37.6 ± 6.5 vs. 5.8 ± 0.7 mean fluorescence, *P* = 0.039; and 22.4 ± 3.8 vs. 6.9 ± 1.6 mean fluorescence, *P* = 0.011). Immunocompetent animals showed a higher infiltration of S100A4+ cells inside the bronchial wall after 28 days, associated with cartilage damage ranging from invasion to complete destruction. *In vitro* expression of S100A4 by human fibroblasts was higher when stimulated by mononuclear cells (MNCs) from BN rats than from RNU (2.9 ± 0.1 vs. 2.4 ± 0.1 mean fluorescence intensity, *P* = 0.005). Similarly, S100A4 was highly expressed in response to human MNCs compared to stimulation by T-cell-depleted human MNCs (4.3 ± 0.2 vs. 2.7 ± 0.1 mean fluorescence intensity, *P* < 0.001). Obliterative bronchiolitis has been induced in a new xenotransplant model in which chronic airway obstruction was associated with immune activation against the xenograft. Cartilage infiltration by S100A4+ cells might be stimulated by T cells.

*Transplant International* 2016; 29: 1337–1348

## Key words

chronic rejection, humanized model, lung transplantation, S100A, T cells

Received: 1 April 2016; Revision requested: 30 May 2016; Accepted: 29 August 2016; EV Pub Online 4 October 2016

## Introduction

Lung transplantation (LTx) is considered as the last resort treatment for end-stage pulmonary disease. However, it provides the patient with the lowest long-term survival among all solid organ transplantations with an overall median survival of 5.5 years [1]. Chronic lung allograft dysfunction (CLAD) accounts for 30% of recipients' death at 5 years after LTx and is mainly because of the development of a bronchiolitis obliterans syndrome (BOS). The progressive airway obstruction, unexplained by acute rejection, infection, or other confounding complications, affects 49% and 75% of recipients by 5 and 10 years post-LTx, respectively. An irreversible decline in pulmonary function tests is observed with a significant decrease in the forced expiratory volume in second.

The exact mechanism by which BOS occurs is still unknown even if an immune-mediated process has been strongly suggested [2,3]. Repeated acute cellular rejections are known to be strong predictors of CLAD. Several nonimmunological factors have also been reported to be linked to BOS development such as cytomegalovirus infections, gastroesophageal reflux, respiratory viral infections, and pneumonitis because of *Pseudomonas aeruginosa* [4]. Despite a wide heterogeneity of risk factors, chronic airway rejection is characterized by a relatively homogenous phenotype among LTx recipients regarding time of onset, histological features, disease severity, and lack of response to treatment [5]. To date, there is neither relevant preventive strategy to improve long-term outcomes, nor efficient therapy to reverse established BOS [6].

Increased level of S100 family protein expression in fibroblasts has been reported in patients suffering from CLAD [7]. A recent clinical study showed that the level of S100 proteins in the bronchoalveolar lavage fluid varied according to the phenotype of CLAD [8]. Among the multigene calcium-binding S100 protein family, the S100A4 protein is usually expressed by fibroblasts and immune cells [9]. Overexpression of the S100A4 protein, also known as metastatin or calvasculin, has been identified in many malignant tumors and is associated with a more aggressive phenotype in these cancers [9,10]. The expression of S100A4 in the fibroproliferative lesions observed after LTx has not been investigated and might represent a new biomarker of obliterative bronchiolitis (OB).

Since the first description of OB following combined heart–lung transplantation in the mid-1980s, many

efforts have been made to create a relevant animal model of OAD. The orthotopic tracheal transplantation model has been shown to be more representative of the OB found in human LTx recipients, even if luminal obliteration is moderate and delayed compared to the heterotopic model [11]. This preclinical model provides also excellent opportunities to investigate immunosuppressants' delivery by the route of inhalation [12]. However, rodents do not share the human respiratory histology and immunogenicity, so that the orthotopic animal model cannot closely reproduce human OB pathogenesis and may have a different sensitivity to medical treatment compared to human tissue. In this study, we first developed an original xenotransplant model using human bronchial graft in rats. Then, we investigated the expression of the S100A4 protein in the fibroproliferative disorder that progressively leads to OAD.

## Methods

### Animals

Adult Brown Norway (BN) and nude (RNU) rats, 320–450 g, were purchased from Charles River Laboratories (Sulzfeld, Germany). All animals were housed under normal conditions and received standard rodent food and water, and humane care in compliance with the Guide for the Principles of Laboratory Animals, prepared by the Institute of Laboratory Animal Resources and published by the National Institutes of Health. The animals were maintained in the animal care facilities of the Campus Research from the University Hospital Hamburg-Eppendorf (Hamburg, Germany).

### Study groups

For each strain, animals were randomly assigned to two groups: Animals were sacrificed either at the seventh postoperative day (BN<sub>7</sub> group,  $n = 6$  and RNU<sub>7</sub> group,  $n = 7$ ) or at the 28th postoperative day (BN<sub>28</sub> group,  $n = 6$  and RNU<sub>28</sub> group,  $n = 6$ ).

### Experimental surgery

#### Graft preparation

Distal bronchi of human native lungs were procured from LTx recipients. Lungs with bronchial disease such as cystic fibrosis were excluded. In this study, all

patients had primary pulmonary hypertension, without pulmonary fibrosis, and thus were supposed to have healthy distal bronchi. These donors gave their full, informed, written consent to the study. The experimental protocol was approved by the local ethics committee for animal study using human tissues. The recovered lungs were preserved in a 4 °C medium (RPMI medium; Gibco, Life Technologies GmbH, Paisley, UK), and human bronchi were transplanted to rats in the following 48 h to avoid graft ischemic injuries. Human bronchi were prepared for an equivalent length of a six-ring segment of rat trachea. Careful attention was paid to the airway anatomic polarity of the graft to prevent any disturbance of the mucous clearance. The graft was flushed with cold saline and then stored at 4 °C until the recipient trachea was divided.

#### *Recipient operation*

Orthotopic tracheal transplantation was performed in rats according to the method previously described [11]. The recipient trachea was transversally opened three to four rings caudal from the cricoid cartilage. As the trachea was not distally divided before the proximal graft anastomosis was performed, animals maintained spontaneous ventilation through the tracheostomy thereby avoiding the need for mechanical ventilatory support during the procedure. The human graft was first sutured to the proximal recipient trachea (cervical) by an edge-to-edge method maintaining the anatomic polarity of the human bronchus. The posterior aspect of the anastomosis was performed in continuous running fashion using 8-0 (Prolene, Ethicon, Germany). The anterior aspect was completed using interrupted 8-0 stitches. After airway secretions and clots cleaning, a four-ring segment of the recipient trachea was removed. An edge-to-edge distal suture to the mediastinal trachea was realized in the same fashion than the proximal one.

## **Histopathology**

### *General histology*

See Supporting Information.

### *Immunofluorescence*

See Supporting Information.

## **Immune response assays**

### *ELISPOT assays*

Donor lymphocytes were isolated and counted after mitomycin inhibition ( $1 \times 10^6$  cells/ml, 100  $\mu$ l/well). During graft recovery at Days 7 and 28, recipient's spleen was removed and homogenized and splenocytes were isolated and counted ( $1 \times 10^7$  cells/ml, 100  $\mu$ l/well). Donor's lymphocytes were pooled with recipient's cells. After a 24-hour incubation time at 37 °C, type 1 T-helper (Th-1) response was quantified according to ELISPOT protocol (BD Biosciences, Heidelberg, Germany) using rat interferon- $\gamma$  (IFN- $\gamma$ ). Spots were automatically enumerated using an ELISPOT plate reader (Cincinnati Testing Laboratories, Cincinnati, OH, USA) for scanning and analyzing.

### *Donor-specific antibodies*

Sera from BN and RNU recipients were decomplexed by heating to 56 °C for 30 min and subsequently diluted by 1 of 3 in phosphate-buffered saline containing 3% fetal calf serum and 0.1% NaN<sub>3</sub>. Sera were incubated for 1 h at 37 °C and then mixed with donor cells. Mean fluorescence intensity was measured by flow cytometry using antibodies against human IgM and IgG alloantibodies (AbD Serotec, Dusseldorf, Germany). Mean fluorescence emission of sera from naïve BN rats served as reference and was set to 1000. Data were analyzed using the Flowjo software (Tree Star Inc., Ashland, OR, USA).

## **S100 A4 cell infiltration and cartilage damages**

### *Light microscopy*

See Supporting Information.

### *In vitro assay*

See Supporting Information.

### *Cartilage transplant experiment*

See Supporting Information.

## **Statistical Analysis**

Results are presented as mean value  $\pm$  SD. Comparison between groups was performed by one-way analysis of variance with least significant difference *post hoc* test.

$P < 0.05$  was considered statistically significant. All analyses were performed using SPSS software (Statistical Package for the Social Sciences, version 17.0; SPSS Inc., Chicago, IL, USA).

## Results

### Chronic obliterative airway disease in the xenotransplant model

Microscopic examination revealed enhanced mononuclear graft infiltration in the BN group. Severe signs

of chronic rejection in the BN group were observed on Day 28 with interstitial and peribronchiolar fibrosis resulting in marked airway obstruction. Nude animals also showed fibroproliferative lesions but only involving the submucosal area, between the cartilage ring and the epithelial layer (Fig. 1a). The histomorphology of 28-day xenografts in BN rats was similar to that of human BOS samples. Thus, the main pathologic features of human airway allograft chronic rejection can be reproduced in this model (Fig. 1a). The origin of epithelial cells and proliferating cells was human as confirmed by confocal immunofluorescence staining with HLA-I

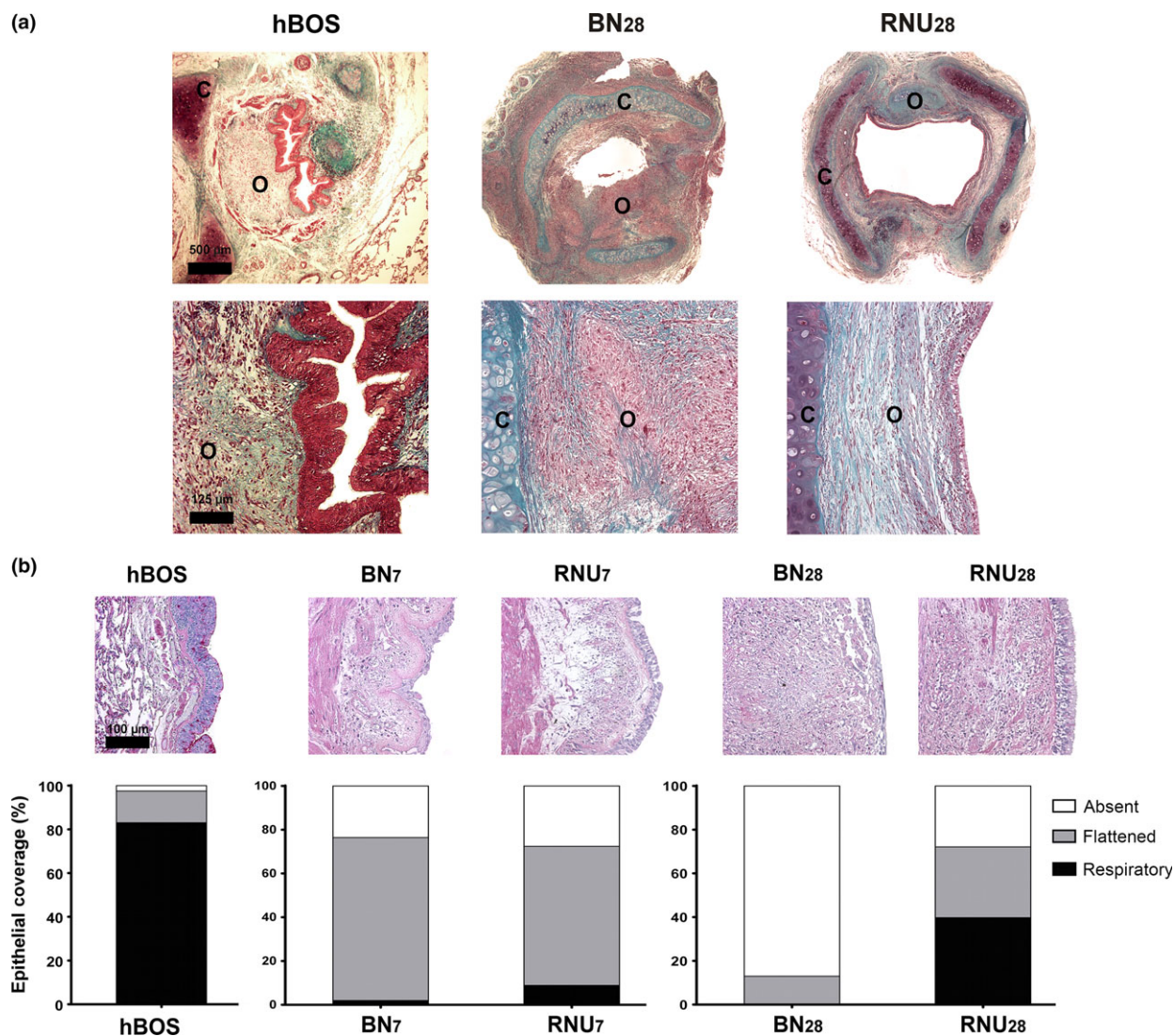


**Figure 1** Development of obliterative airway disease after transplantation. (a) Comparative overview of the obliterative lesion observed in human bronchiolitis obliterans syndrome (BOS), Brown Norway (BN), and nude (RNU) models (trichrome staining, upper pictures). The fibroproliferative disorder seems to be more severe in the BN model (trichrome staining, lower pictures). (b) The composition of the epithelial coverage is reported in human BOS, BN, and RNU model (PAS staining). The physiological epithelium is highly preserved in human patients while it is absent in the BN group and accounts for less than 50% in the RNU group. C: cartilage; O: obliterative lesion.



(Fig. S2). Both BN and RNU animals presented major epithelial destruction within the luminal airway at 7 days after orthotopic tracheal transplantation, without any difference in epithelial coverage categories (Fig. 1b). It may be related to ischemic injury of the epithelial layer. Physiological respiratory epithelium recovered in RNU at Day 28 ( $40\% \pm 17\%$  of epithelial coverage) and was not detectable in BN group ( $P = 0.009$ ). Epithelial layer denudation was more severe in BN group at Day 28 compared to nude animals ( $87\% \pm 7\%$  vs.  $28\% \pm 13\%$ ,  $P = 0.005$ ). There was no significant difference in flattened cuboidal rate between BN and RNU groups at Day 28 (respectively,  $13\% \pm 7\%$  vs.  $32\% \pm 13\%$ ,  $P = 0.319$ ). The epithelial layer was preserved in the bronchi of BOS patients as  $83\% \pm 17\%$  of the luminal circumference included a physiological epithelium (Fig. 1b).

### ***In vivo* immune activation**

#### *Inflammatory cell infiltration*

CD3<sup>+</sup> cell infiltration of the xenograft was higher at Day 28 in the BN group compared to nude animals ( $33\% \pm 10\%$  vs.  $6\% \pm 4\%$ , respectively,  $P < 0.001$ ). There was no difference for CD68<sup>+</sup> macrophage infiltration between BN and RNU groups after 28 days ( $28\% \pm 10\%$  vs.  $30\% \pm 9\%$ , respectively,  $P = 0.487$ ). Human samples showed infiltrating rates of  $18\% \pm 8\%$  and  $13\% \pm 5\%$ , respectively, for CD3<sup>+</sup> cells and CD68 cells (Fig. 2a and b).

#### *ELISPOT assay*

Few spots were detected in the RNU group after ELISPOT analysis. Th-1 mediated a response against the tracheal xenograft which was higher in BN animals compared to nude animals on both Days 7 and 28, as shown by the increased frequencies of donor-reactive IFN- $\gamma$ -producing cells ( $P < 0.001$  and  $P = 0.035$ ). Th-1 immune response was also higher at 7 days compared to 28 days in the BN group (Fig. 2c).

#### *Donor-specific antibodies' detection*

Xenoreactive antibodies of the IgM type were significantly higher at Day 7 after transplant in the BN group compared to RNU ( $37.6 \pm 6.5$  vs.  $5.8 \pm 0.7$  mean fluorescence,  $P = 0.039$ ). Increase in IgG serum level was also significantly higher in the BN group after 28 days ( $22.4 \pm 3.8$  vs.  $6.9 \pm 1.6$  mean fluorescence,  $P = 0.011$ ) (Fig. 2d).

### **Infiltration of S100A4-positive cells associated with cartilage damages in the bronchial graft**

Infiltration of S100A4<sup>+</sup> cells in the bronchial wall was higher in BN animals compared to RNU after 28 days, especially in the cartilage area (respectively,  $2.8 \pm 0.5$  vs.  $1.3 \pm 0.8$  S100A4-staining score,  $P = 0.006$ ). In the mucosal and submucosal areas, there was a trend for a higher infiltration of S100A4<sup>+</sup> cells in the BN group ( $P = 0.069$  and  $0.058$ , respectively) (Fig. 3). Cartilage areas were preserved in all animals on Day 7 after transplantation, with a trend to a cellular infiltration of the smooth borderline in immunocompetent animals at that time (data not shown). Signs of cartilage destruction were observed in the BN group at Day 28, ranged from small areas of invasion to complete destruction of the transplanted cartilage. The cells invading the cartilage, as well as cells surrounding the cartilage area, were positive for the S100A4 protein. Damaged cartilage areas were partially replaced by connective tissue cells. The RNU group had a lower score of cartilage damages compared to BN after 28 days. Most of bronchial cartilages from RNU animals were completely preserved at that time (Fig. 4).

### **Infiltration of S100A4-positive cells in cartilage transplantation**

Similarly, we observed that the cartilage smooth borderline was preserved on more than 70% of the cartilage circumference among RNU 28 days after subcutaneous cartilage transplant. BN rats showed a higher rate of cartilage damages ( $16.6\% \pm 11.3\%$  vs.  $40.2\% \pm 13.2\%$  for invasion grade,  $P < 0.01$ ; and  $1.8\% \pm 1.2\%$  vs.  $35.6\% \pm 18.2\%$  for infiltration grade,  $P < 0.01$ ). The cells attaching and invading the damaged cartilages were highly positive for S100A4 protein. Multiple areas of infiltration associated with remodeling of the cartilage matrix were observed at a similar rate on right and left sides of BN recipients (respectively,  $39.2\% \pm 13.9\%$  vs.  $41.1\% \pm 12.8\%$  for invasion,  $P = 0.91$ ; and  $33.7\% \pm 18.6\%$  vs.  $37.6\% \pm 18.6\%$  for infiltration,  $P = 0.85$ ) (Fig. 5).

### **T-cell-mediated expression of S100A4 protein in human fibroblasts**

*In vitro* expression of S100A4 protein in human fibroblasts was observed with or without T-cell stimulation. MNCs were isolated from rats and from human blood. The mean fluorescence intensity from each sample was normalized by the intensity measured on native human

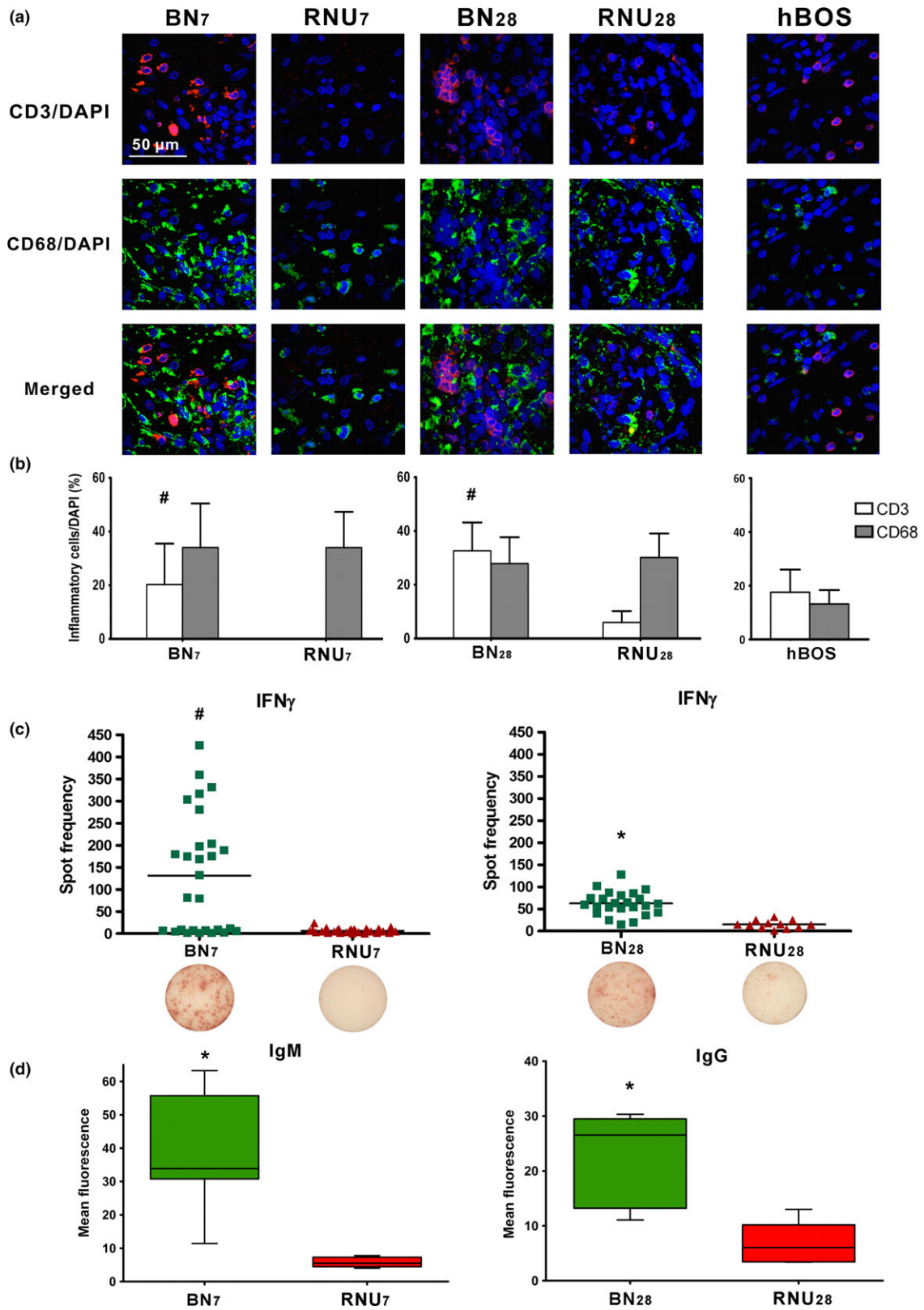


**Figure 2** \* and # explain significant difference between BN and RNU groups with a  $P$  value  $<0.05$  and  $<0.01$  respectively. *In vivo* immune activation after transplantation. (a) Infiltration of CD3- and CD68-positive cells revealed by immunofluorescence staining in Brown Norway (BN) and nude (RNU) models and in human bronchiolitis obliterans syndrome (BOS). (b) Quantification of CD3 and CD68 cells among the cellular population of the bronchial wall (CD3/DAPI and CD68/DAPI ratios). (c) Th1 immune response at seven and 28 days after transplant in BN and RNU models. (d) Donor-specific antibodies (DSA) in the peripheral blood at Day 7 (IgM) and Day 28 (IgG) in both groups.

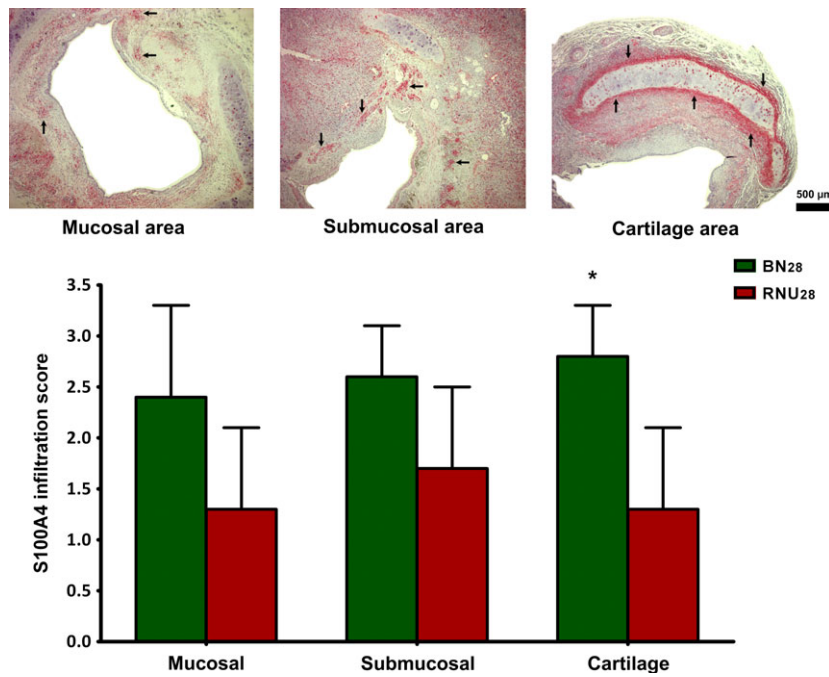


**Figure 3** Infiltration of S100A4-positive cells in the wall of bronchial allografts. The bronchial wall was divided into mucosal, submucosal, and cartilage areas. Bronchial graft infiltration by S100A4-positive cells (black arrows) was higher in Brown Norway (BN)<sub>28</sub> compared to nude (RNU)<sub>28</sub>, especially in the cartilage area. \* explains significant difference of S100A4 infiltration between BN<sub>28</sub> and RNU<sub>28</sub> with a *P* value < 0.05 (immunohistochemistry staining for human S100A4 protein, ×50).

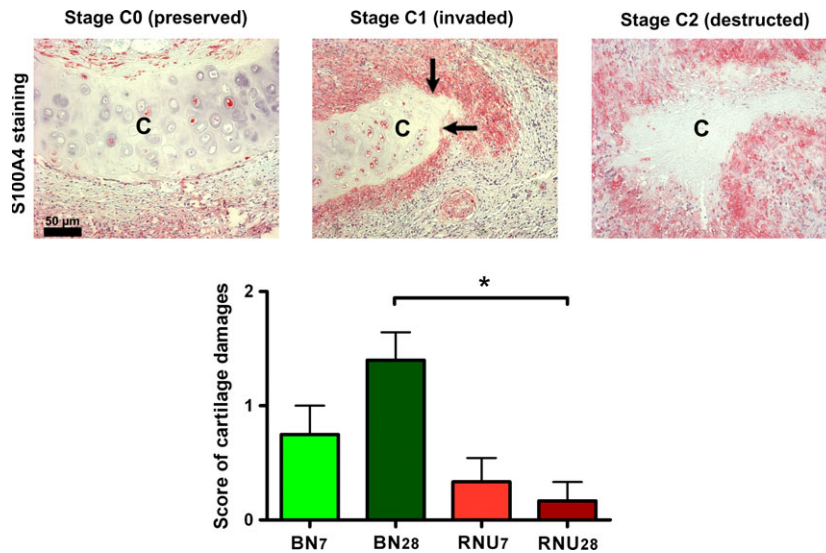


**Figure 4** Cartilage damages of the bronchial allograft in the Brown Norway (BN) and nude (RNU) models. The smooth borderline of the cartilage was analyzed and reported either respected (stage C0) or invaded (stage C1, black arrows). Complete infiltration of the cartilage area associated with partial or complete destruction of the cartilage defined stage C2. For each sample, the maximum score was recorded for semi-quantification of cartilage damages. The cartilage damages were more severe in BN than in RNU and also more important at 28 days compared to seven days. C means cartilage. \* explains significant difference in cartilage damages between BN<sub>28</sub> and RNU<sub>28</sub> with a *P* value < 0.05 (immunohistochemistry staining for human S100A4 protein, ×50).

fibroblasts without MNCs. After addition of MNC from RNU lacking T cells, S100A4 expression highlighted by immunofluorescence was lower compared to culture

slides of human fibroblasts pooled with MNCs from BN rats (respectively,  $2.4 \pm 0.1$  vs.  $2.9 \pm 0.1$  fluorescence intensity, *P* = 0.005). Similarly, stimulation of fibroblasts

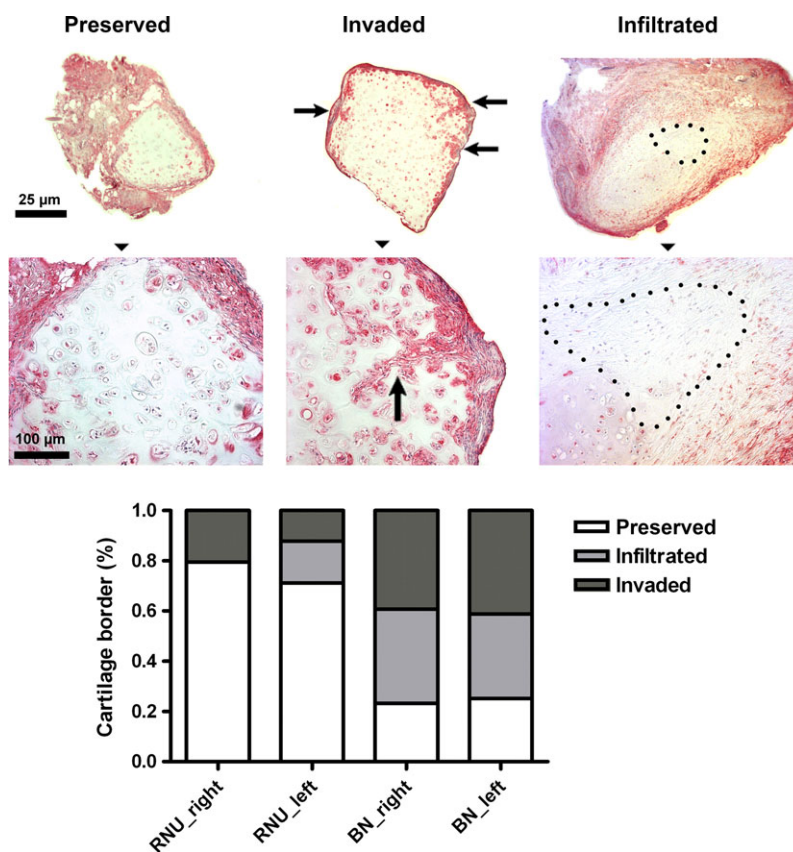


**Figure 5** Damages of the cartilage borderline at 28 days after subcutaneous transplantation in rats. The black arrows show invasion of the human cartilage by S100A4-positive cells (red staining). The cartilage was mainly preserved among nude (RNU) animals whereas it was either invaded or infiltrated in Brown Norway (BN) rats. Loss of cartilage architecture was observed in case of major infiltration of the graft in BN rats (black dots) (immunohistochemistry staining for human S100A4 protein,  $\times 50$  on the upper line,  $\times 400$  on the lower line).

by human MNCs lacking CD3+ cells resulted in a significantly lower mean fluorescence intensity compared to stimulation with nondepleted MNCs ( $2.7 \pm 0.1$  vs.  $4.3 \pm 0.2$  fluorescence intensity,  $P < 0.001$ ) (Fig. 6). Characterization by flow cytometry of human CD3-depleted MNCs is displayed in Figure S3.

### Discussion

We report a new xenograft animal model reproducing the characteristics of OB. The main findings of this study are twofold. First, S100A4 protein is highly expressed in the lesions of OAD observed in transplanted rats and is associated with cartilage damages of the bronchial xenograft. Second, we show that the expression of S100A4 in human fibroblasts is stimulated by T cells both *in vitro* and *in vivo*.

Human OB is a primary disease of distal bronchi after LTx. To be close to this pulmonary obstructive physiology, we chose to transplant a human distal bronchus rather than doing the classic model of orthotopic tracheal

transplant between rats. Fibroproliferative lesions narrowing the bronchial lumen were observed in our model after 28 days. This model may reproduce the pathogenesis of the human OB with the immunological limitation of interspecies cross-reactivity. However, anti-human-specific antibodies are not present in immunocompetent rats. In the present study, immunocompetent animals showed a higher degree of luminal xenograft obliteration compared to nude rats. The orthotopic tracheal transplantation was preferred to the heterotopic model to preserve the airflow continuity of the bronchial graft. Our group previously demonstrated the advantages of the orthotopic tracheal preclinical model compared to the heterotopic model in rats [13,14]. As inhaled drug administration is possible, this model may be useful to investigate inhaled immunosuppressant therapy as well as innovative therapy targeting post-transplant airway disease. Moreover, we presume that our histological findings are close to human features of OB because we used a human xenograft. We found a significant infiltration of lymphocytes and macrophages on Day 28 in the



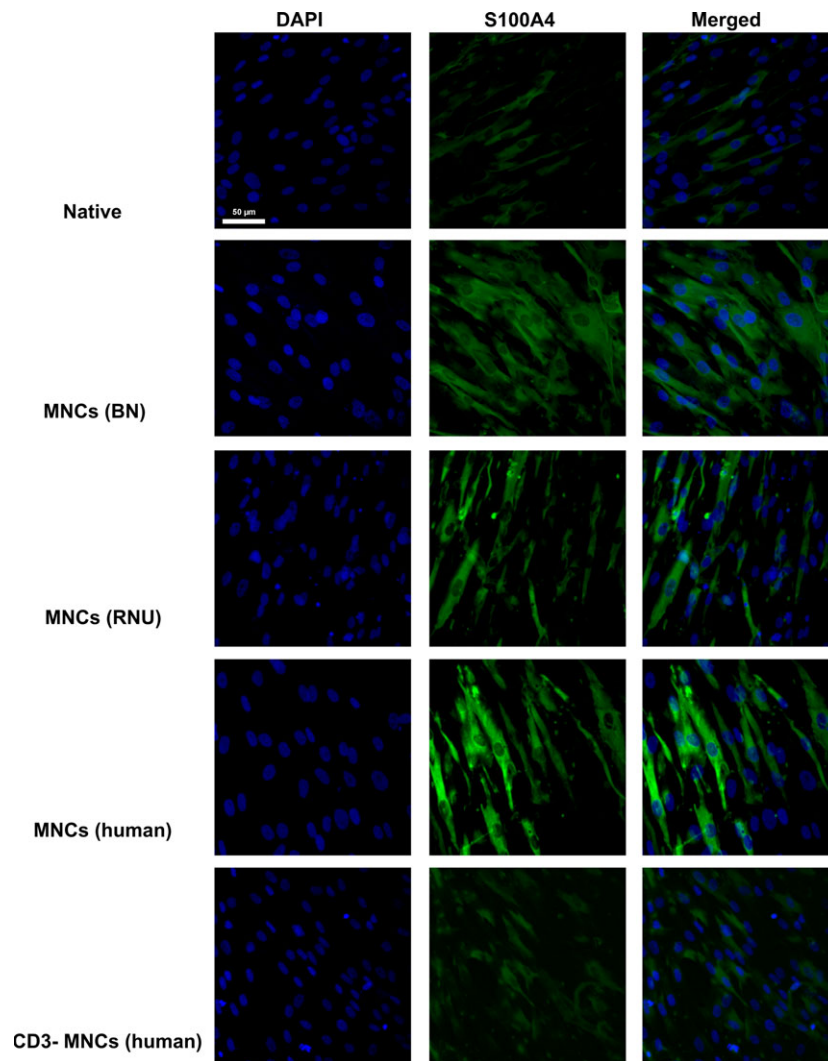


**Figure 6** In vitro expression of S100A4 protein in human fibroblasts. Immunofluorescence intensity of S100A4 protein expressed in human fibroblasts in response to mononuclear cells (MNCs) stimulation is normalized with the basal intensity produced by native human fibroblasts. The expression of S100A4 protein was higher in response to stimulation by MNCs including T cells, both in rat and human experiments (immunofluorescence staining for human S100A4 protein,  $\times 400$ ).

bronchial graft of the BN group associated with a stronger Th-1 immune response as well as the presence of donor-specific antibodies (DSA). Although the epitope targets of these DSA are unknown, the increase in host humoral and cellular responses suggests an immune-mediated process for the OAD observed in our study. All of these experimental findings support evidence for using this preclinical xenotransplant model to further investigate the pathophysiology and response to therapy of the human OB.

Moreover, we observed a significantly higher amount of S100A4<sup>+</sup> cells in the bronchial graft of rats that developed OAD after transplantation. As all donors were free from pulmonary fibrosis, we hypothesized that the expression of S100A4 was not

influenced by transmitted fibrotic lesions. Yousem *et al.* [7] first observed that heart–lung transplant recipients with BOS had a significant increase of dendritic cells expressing S100 proteins in the epithelial layer of the airway conduct. Our findings are also in accordance with a recent report from the Toronto’s group suggesting that the family of S100 proteins detected in the fluid after bronchoalveolar lavage may help to discriminate the different subtypes of CLAD [8]. To our knowledge, we report for the first time that S100A4 is highly expressed experimentally in OAD lesions. Furthermore, we observed a nonexpected histological characteristic associated with OAD in our model. The S100A4<sup>+</sup> cells partially or completely engulfed the cartilage areas of the bronchial

graft 4 weeks after transplantation. The S100A4 protein has previously been established as a regulator of metalloproteinases and cytoskeleton activities in solid malignancies, including lung cancer [10,15–18]. Recently, Stewart *et al.* [10] reported *in vitro* experiments showing that S100A4 blockage is associated with reduced proliferation and decreased invasion in a large panel of lung cancer cell lines. The authors used niclosamide, a well-known antihelminthic agent, to inhibit S100A4 signaling with promising results. Li and colleagues also demonstrated that S100A4 protein mediates macrophage recruitment and chemotaxis *in vivo* [19]. The S100A4 protein is upregulated in tissues exposed to chronic inflammation and may promote the progression of arthritis through cartilage destruction [20]. The S100A4 protein is absent in normal lung tissues and is expressed by a median of 15% (0–48%) of normal epithelial cells in the lung of stable transplanted patients [21]. In a model of pulmonary fibrosis, most of S100A4+ fibroblasts involved in the disease derived from the epithelial lineage via the epithelial–mesenchymal transition (EMT) [22]. By its interactions with cytoskeleton components, S100A4 is one of the main proteins supposed to promote the EMT. The cross talk between epithelial cells and stromal fibroblasts has been implicated in the pathogenesis of OB after LTx, and S100A4 might be associated with abnormal wound repair after epithelial injury [23]. The cartilage injuries were only observed in immunocompetent animals on Day 28 after transplantation in the present study, suggesting that the destructive capability of S100A4+ cells was mediated by T cells. This hypothesis was confirmed by our *in vitro* experiments. The S100A4 protein was more expressed in human fibroblasts secondary to the stimulation by rat or human MNCs, than in fibroblasts exposed to MNCs depleted of CD3+ cells. The S100A4 protein has also been demonstrated to be a marker of T-cell-mediated EMT in chronic allograft rejection after liver and kidney transplantations [24,25]. In our BN model, the physiological respiratory epithelium was absent in animals showing a high rate of S100A4+ cells inside the bronchial wall after 28 days. Airway epithelium is actually known to play an important role in OB development after LTx [26]. The precise mechanism by which repeated epithelial injuries lead to aberrant wound repair is unknown. The lower quality of bronchial wound healing however contributes to the development of EMT, and OB may play a key role in late allograft dysfunction in the setting of solid organ transplant. Upregulation of mesenchymal proteins such as fibronectin, vimentin, and S100A4 might be associated with increased cellular motility and extracellular matrix remodeling during EMT [27]. Our study may further

provide a rationale to target S100A4 protein in the setting of OAD.

Our experimental results also suggest that cartilage damages after transplantation are potentially mediated by S100A4-positive cells resulting from the donor lung and activated by chronic rejection of the allograft. We cannot exclude that ischemia may in part explain the cartilage destruction. However, cartilage areas were preserved in all animals on Day 7, suggesting that any cellular death related to ischemia occurred early after tracheal transplantation. As we observed a similar degree of cartilage lesions on both sides after subcutaneous transplant, the isolated transplanted cartilage might be invaded by S100A4 cells from the contralateral flank. This long-distance *in vivo* migration spreading a cartilage disease has been previously reported by Lefevre *et al.* [28]. They observed a similar rate of cartilage destruction after subcutaneous cotransplantation of human healthy cartilage together with synovial fibroblasts from patients with rheumatoid arthritis compared to isolated cartilage transplant [28]. Interestingly, fibroblasts have also been described as causing cartilage destruction in granulomatosis with polyangiitis [29]. Hence, a common pathophysiological mechanism might be responsible for this destruction in several disease entities. Therefore, S100A4 may be a potential protein biomarker of OB after LTx and might help to develop targeted molecular therapies.

### Authorship

JG: conceived the experiments, carried out experiments, analyzed data, and was involved in writing the paper. RI, MS and XH: carried out experiments and analyzed data. TD: conceived experiments, analyzed data, and was involved in writing the paper. SU: carried out experiments and analyzed data. EF, PD, RCR and HR: conceived the experiments and were involved in writing the paper. US and SS: conceived the experiments, analyzed data, were involved in writing the paper, and secured funding. All authors had final approval of the submitted and published versions.

### Funding

The authors have declared no funding.

### Conflict of interest

There are no financial or personal relationships that might bias this work for each author.

## Acknowledgements

We thank Christiane Pahrman for her technical assistance. We extend special thanks to the UKE Imaging Facility (UMIF, Bernd Zobiak) and the UKE Animal Facility. This study was supported by the Else-Kröner-Fresenius-Stiftung (2012\_EKES.04; T.D.), a grant from the Fondation Leducq (CDA 2013-2015; S.S.), and by the German Research Foundation (Deutsche Forschungsgemeinschaft; DFG: SCHR992/3-1 and SCHR992/4-1; S.S.).

## SUPPORTING INFORMATION

Additional Supporting Information may be found online in the supporting information tab for this article:

### Appendix S1. Methods.

**Figure S1.** Classification of epithelial coverage in the bronchial allograft.

**Figure S2.** Origin of the cells in the fibroproliferative lesions observed after transplantation.

**Figure S3.** FACS analysis of human mononuclear cells (MNCs) used for *in vitro* stimulation of human fibroblasts.

**Video Clip S1.** This video demonstrates the transplantation of human bronchi into the tracheal position of rats as preclinical *in vivo* research model to study pathobiological and pathophysiological processes in the development of OAD.

## REFERENCES

- Christie JD, Edwards LB, Kucheryavaya AY, *et al.* The Registry of the International Society for Heart and Lung Transplantation: twenty-seventh official adult lung and heart-lung transplant report—2010. *J Heart Lung Transplant* 2010; **29**: 1104.
- Schrepfer S, Deuse T, Sydow K, Schafer H, Detter C, Reichenspurner H. Tracheal allograft transplantation in rats: the role of different immunosuppressants on preservation of respiratory epithelium. *Transplant Proc* 2006; **38**: 741.
- Evers A, Atanasova S, Fuchs-Moll G, *et al.* Adaptive and innate immune responses in a rat orthotopic lung transplant model of chronic lung allograft dysfunction. *Transpl Int* 2015; **28**: 95.
- Kotloff RM, Thabut G. Lung transplantation. *Am J Respir Crit Care Med* 2011; **184**: 159.
- Verleden GM, Vos R, Vanaudenaerde B, *et al.* Current views on chronic rejection after lung transplantation. *Transpl Int* 2015; **28**: 1131.
- Krueger T, Berutto C, Aubert JD. Challenges in lung transplantation. *Swiss Med Wkly* 2011; **141**: w13292.
- Yousem SA, Ray L, Paradis IL, Dauber JA, Griffith BP. Potential role of dendritic cells in bronchiolitis obliterans in heart-lung transplantation. *Ann Thorac Surg* 1990; **49**: 424.
- Saito T, Liu M, Binnie M, *et al.* S100 Family proteins in human chronic lung allograft dysfunction: potential markers for biologic subtyping. *J Heart Lung Transplant* 2013; **32**: S60.
- Salama I, Malone PS, Mihaimed F, Jones JL. A review of the S100 proteins in cancer. *Eur J Surg Oncol* 2008; **34**: 357.
- Stewart RL, Carpenter BL, West DS, *et al.* S100A4 drives non-small cell lung cancer invasion, associates with poor prognosis, and is effectively targeted by the FDA-approved anti-helminthic agent niclosamide. *Oncotarget* 2016; **7**: 34630.
- Schrepfer S, Deuse T, Hoyt G, *et al.* Experimental orthotopic tracheal transplantation: the Stanford technique. *Microsurgery* 2007; **27**: 187.
- Schrepfer S, Deuse T, Reichenspurner H, *et al.* Effect of inhaled tacrolimus on cellular and humoral rejection to prevent posttransplant obliterative airway disease. *Am J Transplant* 2007; **7**: 1733.
- Deuse T, Schrepfer S, Reichenspurner H, *et al.* Techniques for experimental heterotopic and orthotopic tracheal transplantations – when to use which model? *Transpl Immunol* 2007; **17**: 255.
- Hua X, Deuse T, Tang-Quan KR, Robbins RC, Reichenspurner H, Schrepfer S. Heterotopic and orthotopic tracheal transplantation in mice used as models to study the development of obliterative airway disease. *J Vis Exp* 2010; **35**. <http://www.jove.com/index/Details.stp?ID=1437>, doi: 10.3791/1437
- Mathisen B, Lindstad RI, Hansen J, *et al.* S100A4 regulates membrane induced activation of matrix metalloproteinase-2 in osteosarcoma cells. *Clin Exp Metastasis* 2003; **20**: 701.
- Flatmark K, Pedersen KB, Nesland JM, *et al.* Nuclear localization of the metastasis-related protein S100A4 correlates with tumour stage in colorectal cancer. *J Pathol* 2003; **200**: 589.
- Bjornland K, Winberg JO, Odegaard OT, *et al.* S100A4 involvement in metastasis: deregulation of matrix metalloproteinases and tissue inhibitors of matrix metalloproteinases in osteosarcoma cells transfected with an anti-S100A4 ribozyme. *Cancer Res* 1999; **59**: 4702.
- Chen N, Sato D, Saiki Y, Sunamura M, Fukushima S, Horii A. S100A4 is frequently overexpressed in lung cancer cells and promotes cell growth and cell motility. *Biochem Biophys Res Commun* 2014; **447**: 459.
- Li ZH, Bresnick AR. The S100A4 metastasis factor regulates cellular motility via a direct interaction with myosin-IIA. *Cancer Res* 2006; **66**: 5173.
- Yammani RR. S100 proteins in cartilage: role in arthritis. *Biochim Biophys Acta* 2012; **1822**: 600.
- Ward C, Forrest IA, Murphy DM, *et al.* Phenotype of airway epithelial cells suggests epithelial to mesenchymal cell transition in clinically stable lung transplant recipients. *Thorax* 2005; **60**: 865.
- Degryse AL, Tanjore H, Xu XC, *et al.* Repetitive intratracheal bleomycin models several features of idiopathic pulmonary fibrosis. *Am J Physiol Lung Cell Mol Physiol* 2010; **299**: L442.
- Hodge S, Holmes M, Banerjee B, *et al.* Posttransplant bronchiolitis obliterans syndrome is associated with bronchial epithelial to mesenchymal transition. *Am J Transplant* 2009; **9**: 727.
- Rygiel KA, Robertson H, Willet JD, *et al.* T cell-mediated biliary epithelial-to-mesenchymal transition in liver allograft rejection. *Liver Transpl* 2010; **16**: 567.
- Robertson H, Ali S, McDonnell BJ, Burt AD, Kirby JA. Chronic renal allograft dysfunction: the role of T cell-mediated tubular epithelial to mesenchymal cell transition. *J Am Soc Nephrol* 2004; **15**: 390.

26. Alho HS, Salminen US, Maasilta PK, Paakko P, Harjula AL. Epithelial apoptosis in experimental obliterative airway disease after lung transplantation. *J Heart Lung Transplant* 2003; **22**: 1014.
27. Kalluri R, Neilson EG. Epithelial-mesenchymal transition and its implications for fibrosis. *J Clin Invest* 2003; **112**: 1776.
28. Lefevre S, Knedla A, Tennie C, *et al.* Synovial fibroblasts spread rheumatoid arthritis to unaffected joints. *Nat Med* 2009; **15**: 1414.
29. Kesel N, Kohler D, Herich L, *et al.* Cartilage destruction in granulomatosis with polyangiitis (Wegener's granulomatosis) is mediated by human fibroblasts after transplantation into immunodeficient mice. *Am J Pathol* 2012; **180**: 2144.